ACS Sustainable Chemistry & Engineering

Research Article

Cite This: ACS Sustainable Chem. Eng. 2018, 6, 9893−9902

Poly(neopentyl glycol 2,5-furandicarboxylate): A Promising Hard Segment for the Development of Bio-based Thermoplastic Poly(ether-ester) Elastomer with High Performance

Dequan Chi,[†,‡] Fei Liu,[*,†] Haining Na,[*,†] Jing Chen,[†] Chuncheng Hao,[‡] and Jin Zhu[†]

[†]Key Laboratory of Bio-based Polymeric Materials of Zhejiang Province, Ningbo Institute of Materials Technology and Engineering, Chinese Academy of Sciences, 1219 Zhongguan West Road, Ningbo 315201, China

[‡]College of Materials Science and Engineering, Qingdao University of Science and Technology, 53 Zhengzhou Road, Qingdao 266042, China

Supporting Information

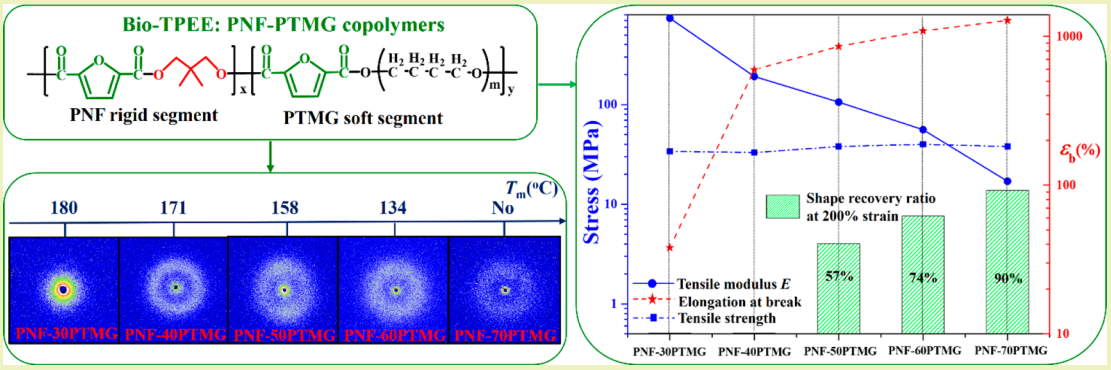

ABSTRACT: With a high melting temperature and good crystallization ability, poly(neopentyl glycol 2,5-furandicarboxylate) (PNF), a polyester derived from bio-based 2,5-furandicarboxylic acid and neopentyl glycol, has been proposed and proved to be a promising hard segment for the development of novel bio-based thermoplastic poly(ether-ester) elastomer (TPEE). The resulting TPEE, namely PNF−PTMG, has high performance comparable to the petroleum-based counterpart PBT−PTMG (i.e., Hytrel, Dupont). Among all of the existing polyesters derived from bio-based 2,5-furandicarboxylic acid (FDCA), PNF has perfectly balanced properties, namely, a high melting temperature of 200 °C and a good crystallization ability to easily grow medium to large-size crystalline spherulites. Characterizations based on dynamic mechanical analysis and small-angle X-ray scattering suggest that there are two domains in PNF−PTMG, the crystalline PNF and a mixture of amorphous PNF and PTMG. These two domains form microphase separation induced mainly by the crystallization of PNF. By adjusting the PTMG soft segment from 30 to 60 wt%, PNF−PTMG shows a melting temperature, tensile modulus (E), and elongation at the break (ε_b) ranging from 180 to 134 °C, 738 to 56 MPa, and 38 to 1089%, respectively. More importantly, the shape recovery ratios increase from 57 to 90% at 200% strain when the amount of PTMG increases from 50 to 70 wt%, indicating excellent elastic property. These results indicate that PNF is an excellent hard segment to serve as a strong physical cross-link so that PNF−PTMG is able to display high performance comparable to extensively commercialized PBT−PTMG.

KEYWORDS: *2,5-Furandicarboxylic acid, Neopentyl glycol, Thermoplastic poly(ether-ester) elastomers, Bio-based, Microphase separation*

INTRODUCTION

Thermoplastic poly(ether-ester) elastomers (TPEEs), with excellent mechanical properties and chemical and heat resistance, are widely used in automotive, medical equipment, communication equipment, and aerospace fields.[1] Usually, TPEEs contain two segments. One is the semi-crystalline polyester hard segment with a high melting temperature and excellent crystallization ability, and the other one is the amorphous polyether soft segment with a low glass transition temperature.[2−4] The crystallization of semi-crystalline polyester induces a microphase separation of the hard segment with the soft one. The microphase separation results in the rigid hard segment serving as a physical cross-link, and the flexible soft part acts as a reversible network. Therefore, the thermal, mechanical, and biodegradation behaviors of TPEEs can be finely regulated by the type and ratio of the hard and soft parts.[5,6] TPEEs consisting of polybutylene terephthalate (PBT) as the hard segment have been commercialized since

Received: March 10, 2018
Revised: May 29, 2018
Published: June 13, 2018

DOI: 10.1021/acssuschemeng.8b01105
ACS Sustainable Chem. Eng. 2018, 6, 9893−9902

Scheme 1. Synthesis of PNF−PTMG

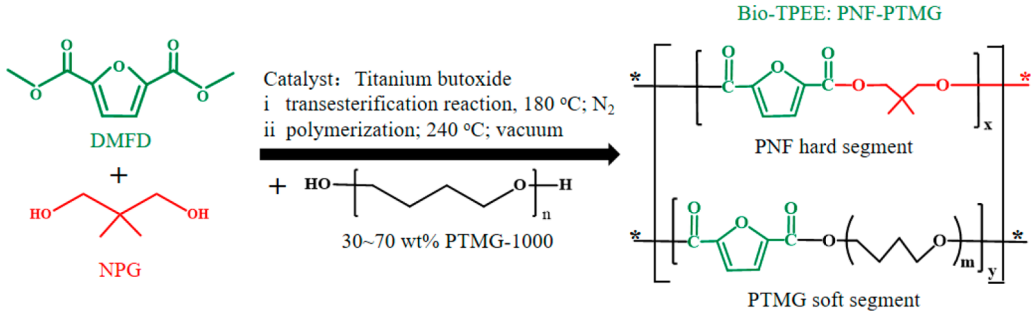

the 1970s (e.g., Hytrel, DuPont),[5] because PBT has a high melting temperature (230 °C) and excellent crystallization ability.

Recently, polymers based on monomers derived from renewable resources have become a high priority because of increasing concerns regarding the depletion of fossil fuels and need for sustainable development.[7−9] Among others, 2,5-furandicarboxylic acid (FDCA), a bio-based monomer that can be derived from renewable resources, such as polysaccharides, starch, and lignocellulosic biomass, has drawn a considerable amount of attention from both academia and industry. It has been considered as a potential alternative to terephthalic acid (TPA) for the synthesis of polymers with high performance, because both of them contain rigid aromatic ring structures. Therefore, FDCA has been applied to the synthesis of semicrystalline aromatic polyesters such as polyethylene 2,5-furandicarboxylate (PEF) and polybutylene 2,5-furandicarboxylate (PBF).[10,11] Polyesters based on FDCA generally have a lower melting temperature but higher glass transition temperature than those of polyesters based on TPA.[10]

Doubtlessly, there is also a strong desire to introduce sustainable monomers for the development of bio-based TPEEs with excellent properties comparable to those of their petroleum-based counterparts.[6−9,12,13] However, simply replacing TPA with FDCA cannot naturally result in good bio-based TPEEs.[14−17] On one hand, the hard segments composed of FDCA-based polyesters have a relatively lower melting temperature or worse crystallization ability than those of the hard segments derived from TPA (e.g., PBT). For example, the melting temperature of PBF is 173 °C, which is nearly 60 °C lower than that of PBT.[18,19] On the other hand, although PEF has a fairly high melting temperature of 220 °C, which is very close to that of PBT, it has a very poor crystallization ability.[20] Therefore, neither PBF or PEF is a good candidate to play as an ideal hard segment for the synthesis of bio-based TPEEs with high performance.[14,17] As a result, in order to induce effective microphase separation in FDCA-based TPEEs so that they have a comparable performance to that of the TPA-based TPEEs,[18,21−23] an ideal hard segment developed from FDCA-based polyester with both a high melting temperature and good crystallization ability is crucial. However, with increasing the chain length of the diol, although a series of FDCA-based polyesters have better crystallization ability compared to that of PEF, they have a linearly decreasing melting temperature to lower than 150 °C.[18]

Poly(neopentyl glycol 2,5-furandicarboxylate) (PNF), a novel and eco-friendly polyester derived from FDCA and neopentyl glycol (NPG), has been reported recently.[24] It has a high melting temperature of about 200 °C and a glass transition temperature of about 68 °C.[24,25] In addition, it also has some particular properties, such as good barrier properties, due to its high crystallization ability.[26] These characteristics immediately make PNF an ideal hard segment for the synthesis of TPEEs with high performance. Therefore, in this work, for the very first time, by using PNF as the hard segment and poly(tetramethylene glycol) (PTMG) as the soft segment, we designed and synthesized a novel bio-based TPEE, namely, PNF−PTMG. The chemical structure, composition, microphase separation, thermal and mechanical properties, and elastic properties were systematically investigated. The comparison between PNF−PTMG and other TPEEs is discussed in great detail. We believe that PNF−PTMG represents one of the bio-based TPEEs that have great potential for the substitution of traditional TPEEs.

EXPERIMENTAL SECTION

Materials. Neopentyl glycol (NPG, 99%), poly(tetramethylene glycol) (PTMG) with a number-average molecular weight of 1000 g mol^{-1}, titanium butoxide (≥99.0%), methanol (99.5%), 1,1,1,3,3,3-hexafluoro-2-propanol (HFIP) (99.5%), phenol (AR), and 1,1,2,2-tetrachloroethane (TCE) (98%) were purchased from Aladdin Reagent Co., Ltd. Dimethyl 2,5-furandicarboxylate (DMFD) was purchased from Chem Target Technologies Co., Ltd. (Mianyang, China). Chloroform (HPLC, ≥99.9%) was purchased from Sinopharm Chemical Reagent Co., Ltd. All chemicals were used as received without further purification.

Synthesis of PNF−PTMG. PNF−PTMG copolymers were synthesized via a two-stage melt polymerization (Scheme 1) involving transesterification of DMFD with NPG at 180 °C under N_2, followed by melt polycondensation at 240 °C under vacuum. A typical process for the synthesis of PNF−PTMG (with 50 wt% of PTMG) is described. DMFD (18.42 g, 100.0 mmol), NPG (10.02 g, 96.2 mmol), and PTMG (21.10 g, 21.1 mmol) were introduced into a 250 mL high pressure reactor equipped with an overhead mechanically stirring and distillation device, and titanium(IV) butoxide (9.21 mg, 0.05 wt% of DMFD) was added into the reactor. The reactor was then sealed and applied vacuum (~10 Pa), followed by purging with dry N_2. This cycle was repeated three times to remove air and moisture. Then, the transesterification reaction was conducted at 180 °C for 4 h in N_2 atmosphere. When the amount of methanol collected as a by-product was 99% of the theoretical yield, the reaction temperature was increased to 240 °C and was maintained for 4 h under vacuum below 20 Pa. The PNF homopolymer was synthesized following the same procedure. The produced copolymers were coded as PNF-*a*PTMG, where *a* is the theoretical weight fraction of PTMG ranging from 30 to 70. For example, PNF-50PTMG means that the copolymer contains 50 wt% of PTMG in feed.

Characterization Methods. The structure and the weight fraction of PTMG in the final polymers were determined by proton nuclear magnetic resonance (^{1}H NMR) in $CDCl_3$ solvent using a Bruker AVIII400 NMR spectrometer (400 MHz) at room temperature. Fourier transform infrared spectroscopy (FTIR) was recorded with a Cary660 +620 FT-IR micro infrared spectrometer (Agilent) at

DOI: 10.1021/acssuschemeng.8b01105
ACS Sustainable Chem. Eng. 2018, 6, 9893−9902

room temperature. Number-average molecular weights (M_n) and dispersities ($Đ$) were measured on PL-GPC220 gel permeation chromatography (GPC) instrumentation. The intrinsic viscosities [η] of PNF and PNF−PTMG were determined using a capillary Ubbelohde viscometer (type Ic, K = 0.03294) at 30 °C in phenol−tetrachloroethane (50/50 wt%, Aladdin, AR) solutions. The thermal properties of PNF and PNF−PTMG were measured with differential scanning calorimetry (Mettler-Toledo DSC I) instrument. The thermal stability values were measured using a Mettler-Toledo TGA/DSC thermogravimetric analysis (TGA) instrument. Dynamic mechanical properties were measured using a TA-Q800 dynamic mechanical analyzer (TA Instruments) working in the film tension mold in a temperature range from −110 to 20 °C lower than the melting temperature of the sample, at a frequency of 1 Hz and heating rate of 3 °C min^{-1}. Small angle X-ray scattering (SAXS) measurements were performed on a Xenocs X-ray small angle scatterometer (Xeuss 2.0, France) with a monochromatic radiation of wavelength 0.15 nm. X-ray diffraction (XRD) measurements of the synthesized copolymers were carried out using a D8 advance X-ray diffractometer (Bruker, Germany). Tensile testing and cyclic tensile testing were performed at room temperature (25 °C) using an Instron5567 tensile testing machine with a 500 N load cell, an contact optical long travel extensometer (Zwick, Ulm, Germany), and Bluehill 2 software (Instron, Norwood, MA, USA). Detailed information about the sample treatment and characterization methods can be found in the Supporting Information.

RESULTS AND DISCUSSION

Molecular Structure Characterization. PNF and PNF−PTMG with 30−70 wt% PTMG were synthesized via transesterification and melt polycondensation reactions as shown in Scheme 1. The number-average molecular weights (M_n) and dispersities ($Đ$) of PNF−PTMG with 30−60 wt% PTMG were determined by GPC measurement. These four samples exhibit fairly high M_n ranging from 94000 to 138000 g mol^{-1} (Table 1). Moreover, the unimodal molecular weight distribution is found for these samples as displayed in their GPC profiles (Figure S1). The $Đ$ of the samples ranges from 2.26 to 3.50. However, with chloroform as the solvent, PNF was almost insoluble, while gelation phenomena were observed for PNF-70PTMG. Therefore, we were unable to obtain M_n and $Đ$ for these two samples by using GPC analysis. Instead, we measured the intrinsic viscosity [η] with phenol−tetrachloroethanein as the solvent. As shown in Table 1, the [η] of PNF−PTMG is in the range of 1.12−1.48, while that of PNF is 0.58. Therefore, PNF-70PTMG also has high M_n similar to the rest of the PNF−PTMG samples.

Table 1. Molecular Structure of PNF and PNF−PTMG

sample	PTMG (wt %)	PNF (mol %)	M_n (g mol^{-1})	$Đ$	[η]
PNF	0	100	–	–	0.58
PNF-30PTMG	34	90	105000	2.26	1.31
PNF-40PTMG	45	86	94000	2.43	1.12
PNF-50PTMG	51	83	132000	3.50	1.48
PNF-60PTMG	62	75	138000	2.34	1.46
PNF-70PTMG	71	67	–	–	1.33

The molecular structure of PNF, as well as PNF−PTMG, was confirmed with ^{1}H NMR, which is shown with peak assignments in Figure 1. The signals at chemical shifts (δ) = 7.19 ppm (a), 4.20 ppm (b), and 1.10 ppm (f) can be assigned to the protons of the aromatic furan ring units (−C_4H_2O−), methylene (−CH_2−$C(CH_3)_2$−), and methyl (−$C(CH_3)_2$−) of the NPG repeating blocks, respectively. The signals at δ = 3.40 ppm (e) and 1.60 ppm (h) are the signals of protons of the methylene unit next to the oxygen (−CH_2−CH_2−O−) and the methylene unit in the middle (−CH_2−CH_2−O−) in the PTMG repeating blocks, respectively. The small signals at δ = 4.34 ppm (d) and 1.81 ppm (g) are protons of the methylene unit next to ester bonds (−C(O)−O−CH_2−) in the PTMG repeating blocks. Therefore, the weight fraction of the PTMG soft segment and mole fraction of PNF can be calculated from ^{1}H NMR analysis according to eqs 1 and 2;[14] the results are showed in Table 1. All PNF−PTMG have a PTMG amount that is relatively higher than the feed ones, probably because of the sublimation of NPG during the polycondensation stage.

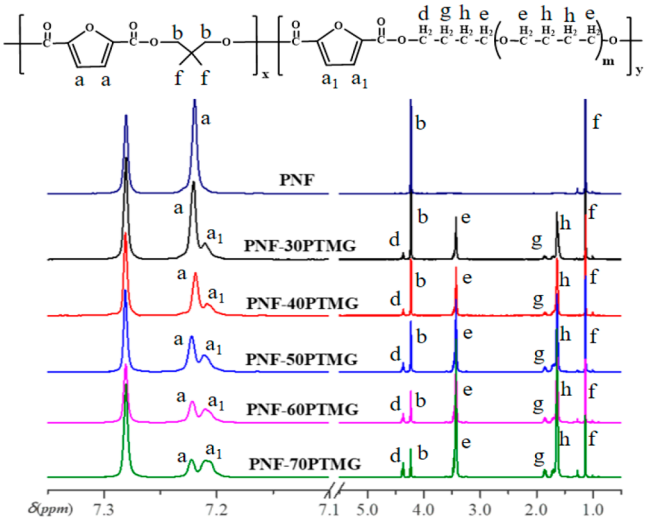

Figure 1. ^{1}H NMR spectra ($CDCl_3$, 400 MHz) of PNF and PNF−PTMG.

$$\text{PTMG wt\%} = \frac{\frac{I_{1.63}}{4} \times 72 + \frac{I_{1.85}}{4} \times 88 + \frac{I_{7.21}}{2} \times 122}{\frac{I_{7.22}}{2} \times 224 + \frac{I_{7.21}}{2} \times 1122} \times 100\% \quad (1)$$

$$\text{PNF mol\%} = \frac{\frac{(1 - \text{PTMG wt\%})}{224}}{\frac{(1 - \text{PTMG wt\%})}{224} + \frac{\text{PTMG wt\%}}{1122}} \times 100\% \quad (2)$$

where $I_{1.63}$, $I_{1.85}$, $I_{7.22}$, and $I_{7.21}$ are designated as the peak intensities of (h), (g), (a), and (a_1), respectively, and their molecular weights were 72 (−$OCH_2CH_2CH_2CH_2$−), 88 (−$OCH_2CH_2CH_2CH_2O$−), 224 (−$OCH_2C(CH_3)_2CH_2O$−$C_6H_2O_3$), and 122 (−$C_6H_2O_3$−), respectively. The PTMG soft segment has a molecular weight of 1122 (−$C_6H_2O_3$−(O−$CH_2CH_2CH_2CH_2)_{(m+1)}$−). The molecular structure of PNF and PNF−PTMG was also confirmed by FT-IR as shown in the Supporting Information (Figure S2).

Thermal Properties. The thermal properties of PNF and PNF−PTMG were investigated by DSC and TGA analysis. Figure 2 shows the DSC curves of PNF and PNF−PTMG in the second heating and cooling scans. The results are summarized in Table 2.

First, the thermal and crystalline behavior is carefully understood and researched. As shown in the second heating

DOI: 10.1021/acssuschemeng.8b01105
ACS Sustainable Chem. Eng. 2018, 6, 9893−9902

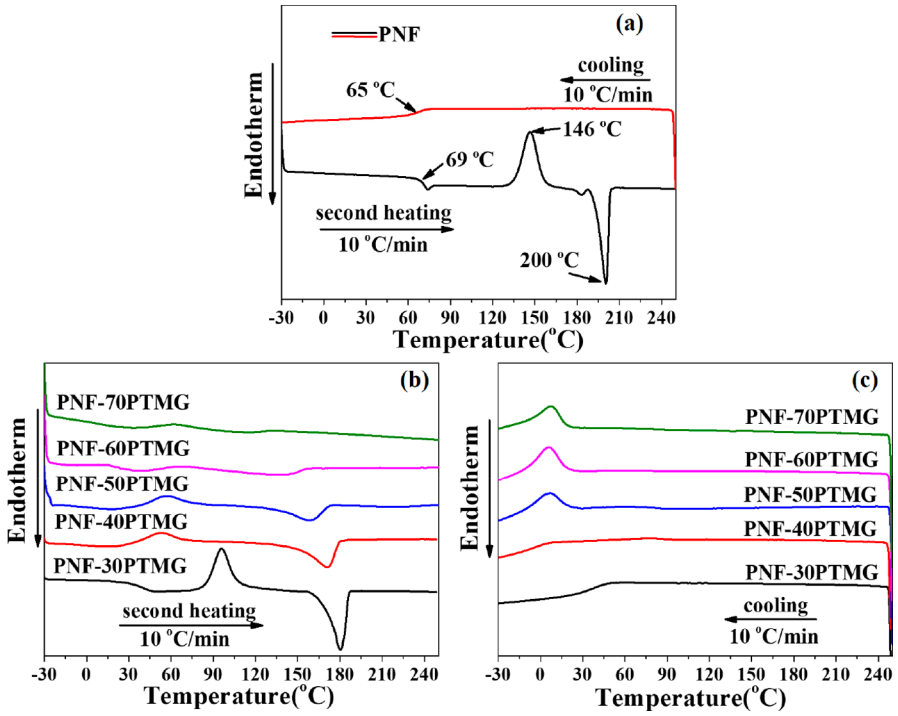

Figure 2. DSC curves of (a) PNF and (b) PNF−PTMG in the second heating scans and (c) cooling scans.

Table 2. Thermal Properties of PNF and PNF−PTMG

sample	T_m (°C)	T_{cc} (°C)	ΔH_m (J g^{-1})	ΔH_{cc} (J g^{-1})	χ_c (%)	T_g (°C)	$T_{5\%}$ (°C)	T_{max} (°C)
PNF	200	146	30.7	32.8	47.7	69	369	407
PNF-30PTMG	180	96	24.4	18.1	31.9	37	321	412
PNF-40PTMG	171	53	20.5	9.3	22.3	–	327	410
PNF-50PTMG	158	57	14.4	8.8	17.4	–	328	404
PNF-60PTMG	134	–	–	–	–	–	336	407
PNF-70PTMG	–	–	–	–	–	–	346	410

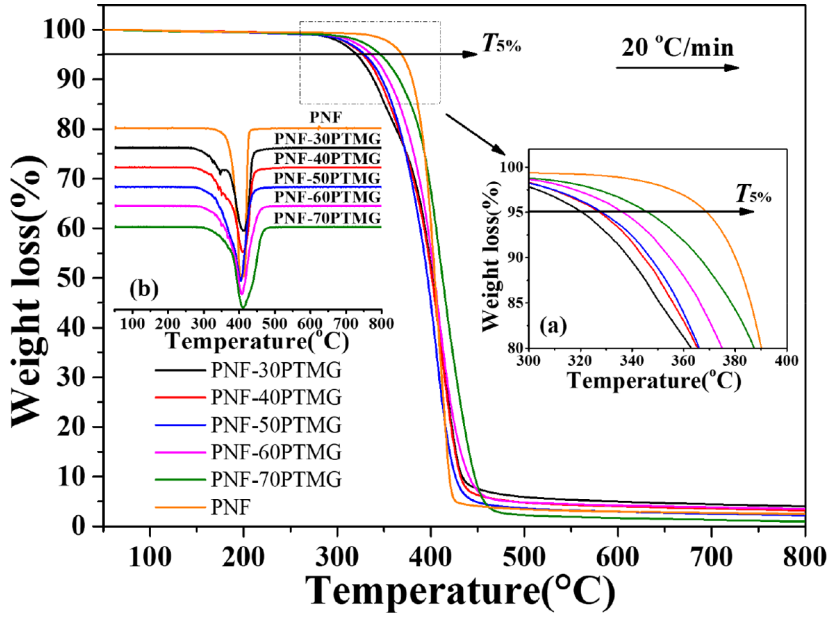

Figure 3. TGA/DTG curves of PNF and PNF−PTMG under N_2 atmosphere.

scan in Figure 2a, PNF has a T_m of 200 °C and a T_{cc} of 146 °C. This result clearly exhibits the high melting point of PNF. As to the crystallization ability of PNF, previous studies have already performed extensive experimental research studies and drawn a clear conclusion. Papageorgiou and co-workers[24] showed that the quenched PNF also showed obvious cold

DOI: 10.1021/acssuschemeng.8b01105
ACS Sustainable Chem. Eng. 2018, 6, 9893−9902

Table 3. Comparison of δ_s Values of PNF, PBF, and PBT with That of PTMG

sample	PNF	PBF	PBT	PTMG
δ_s (J cm^{-3})$^{1/2}$	20.3	22.9	22.7	8.5
$\Delta\delta_s$ (J cm^{-3})$^{1/2}$	11.8	14.4	14.2	–

crystallization during the heating scan at 20 °C min^{-1}, while the semi-crystalline PNF obtained by annealing showed a melting peak at 198.3 °C without cold crystallization behavior. These results were consistent with those of ours in the current study (Figure 2a and Table 2). More importantly, the crystallization ability of PNF is further proved to be better than those of PEF and PPF.[10,19,20,24,27] PNF can crystallize in a wide temperature range, with the fastest crystallization rate at 165 °C.[24] Medium to large crystalline spherulites and a relatively low nucleation density can be observed for PNF, which is favorable for inducing effective microphase separation. In contrast, PEF,[20] PPF,[27] and PBF[19,28] tend to form small spherulites with a relatively high nucleation density.[10] Therefore, we can easily understand that, with fairly high T_m good crystallization ability, PNF would be a promising hard segment among all of the existing FDCA-based polyesters for the development of a novel bio-based TPEE with high performance.

Second, when the PTMG soft segment is incorporated to form a segmented block copolymer, the resulting PNF−PTMG has decreased T_m, T_{cc}, and χ_c values, and all three parameters decrease gradually with an increasing amount of PTMG. When the amount of PTMG is 60 wt%, PNF-60PTMG has no T_{cc}, and when the amount of PTMG is 70 wt%, PNF-70PTMG has no T_m. In other words, PNF−PTMG becomes totally amorphous when the PTMG amount is 70 wt%. Similar trends can also be observed in other TPEE systems, in that

Table 4. T_α of PNF and PNF−PTMG from DMA and Fox Equation

sample	T_α (°C) by DMA	T_α (°C) by Fox equation	ΔT_α (°C)
PNF	71	–	–
PNF-30PTMG	43	0	43
PNF-40PTMG	12	−17	29
PNF-50PTMG	−12	−25	13
PNF-60PTMG	−32	−40	8
PNF-70PTMG	−45	−50	5
PTMG	−78	–	–

with increasing the soft segment amount, the T_m decreases.[29,30] This is due to the depression effect of the non-crystallizable PTMG soft segment on the crystallizable PNF hard segment, which could be quantitatively determined by the Flory equation.[31] Detailed analysis can be found in the Supporting Information. It was found that PNF−PTMG has a similar thermal behavior compared with traditional TPEEs based on TPA, such as PBT−PTMG, and with novel TPEEs based on FDCA, such as PBF−PTMG.

The study of the thermal stability of PNF and PNF−PTMG should not be neglected, as this involves possible decomposition in the material processing and molding process. Therefore, TGA analysis was performed in an N_2 atmosphere. The TGA/DTG curves are shown in Figure 3, and the values for $T_{5\%}$ and T_{max} can be found in Table 2. First, PNF has $T_{5\%}$ of approximately 369 °C, which is relatively higher than that of PBF.[12] Therefore, PNF has excellent thermal stability and can be safely processed at a temperature higher than its melting point. Secondly, when PTMG is incorporated, PNF−PTMG has a decreased $T_{5\%}$ compared with that of PNF. Moreover, with increasing the PTMG amount in PNF−PTMG, $T_{5\%}$ increases slightly. This trend was also observed in the PBF−PTMG series[14] but not in the PBT−PTMG ones.[32] Finally, all

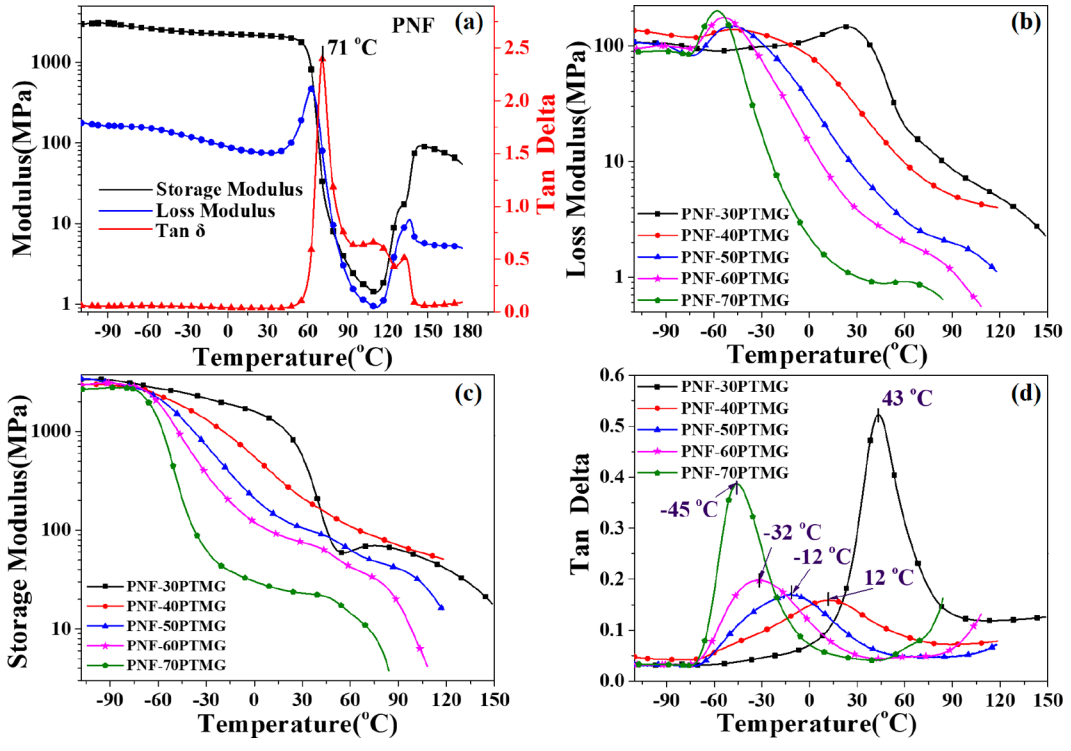

Figure 4. (a) DMA curve of PNF, (b) loss modulus, (c) storage modulus, and (d) mechanical loss tan δ of PNF−PTMG.

DOI: 10.1021/acssuschemeng.8b01105
ACS Sustainable Chem. Eng. 2018, 6, 9893−9902

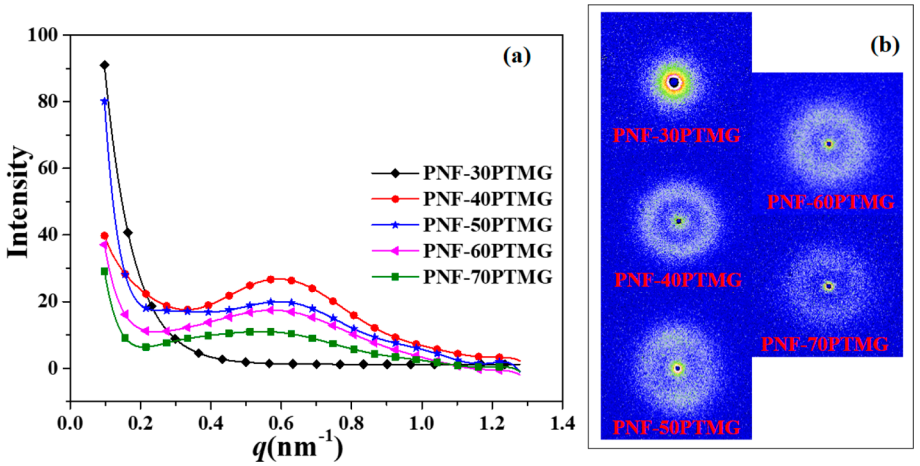

Figure 5. SAXS profiles for PNF−PTMG (a) one-dimensional curves and (b) two-dimensional patterns.

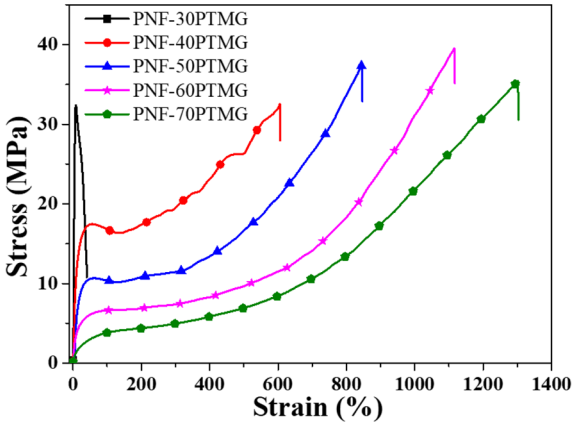

Figure 6. Representative tensile strain−stress curves of PNF−PTMG.

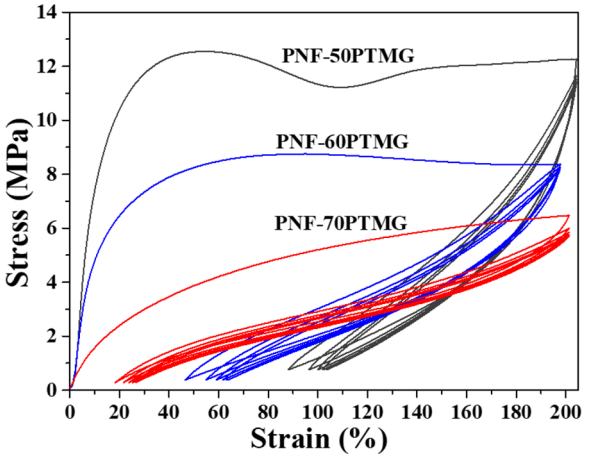

Figure 7. Representative cyclic tensile testing strain−stress curves of PNF−PTMG.

samples have only a single peak in DTG curves, indicating a similar decomposition mechanism, and their T_{max} are within a narrow range from 404 to 412 °C.

Analysis of Microphase Separation. Analysis of the thermal properties of PNF and PNF−PTMG indicates clearly that PNF has a good crystallization ability and fairly high melting temperature and thermal stability. It is therefore crucial to see whether there is microphase separation in PNF−PTMG similar to that in traditional TPEEs such as PBT−PTMG. Generally, the degree of microphase separation is determined by two key factors; one is the thermodynamic factor, mainly the miscibility between the hard segment and soft segment, and the other is the kinetic factor, usually the crystallization of the hard segment.

On one hand, the thermodynamic miscibility between the PNF hard segment and PTMG soft segment can be quantitatively analyzed based on calculations of the solubility parameters (δ_s) of the two components at the molecular level.[33,34] The difference between the δ_s of two polymers ($\Delta\delta_s$) may be considered as the distance between the two polymer chains in a three-dimensional space. A larger $\Delta\delta_s$ indicates worse thermodynamic miscibility, which would result in a greater degree of microphase separation.[35,36] Small has put forward that the δ_s of a polymer can be theoretically predicted by calculating the sum of molar attraction constants (F_i) of each group of repeating structural units (eq 3).[37]

$$\delta_s = \rho \frac{\sum F_i}{M_0} \tag{3}$$

where ρ is the density of the polymer, $\sum F_i$ is the sum of F_i of each group, and M_0 is the relative molecular mass of repeating structural units of the polymer. Therefore, on the basis of eq 3, the δ_s values of PNF as well as PBF and PBT were calculated,

Table 5. Tensile Properties of PNF−PTMG

sample	E (MPa)	σ_t (MPa)	ε_b (%)	σ_y (MPa)	ε_y (%)
PNF-30PTMG	738 ± 19	34 ± 1	38 ± 1	–	–
PNF-40PTMG	192 ± 25	33 ± 3	597 ± 46	14.9 ± 0.3	21 ± 1
PNF-50PTMG	106 ± 9	38 ± 4	857 ± 43	9.3 ± 0.4	27 ± 4
PNF-60PTMG	56 ± 8	40 ± 2	1089 ± 36	–	–
PNF-70PTMG	17 ± 5	38 ± 4	1281 ± 60	–	–

DOI: 10.1021/acssuschemeng.8b01105
ACS Sustainable Chem. Eng. 2018, 6, 9893−9902

Table 6. Elastic Properties of PNF−PTMG[a]

sample	$R_r(1)$ (%)	$R_r(2)$ (%)	$R_r(3)$ (%)	$R_r(4)$ (%)	$R_r(5)$ (%)
PNF-50PTMG	57.1 ± 2.9	92.7 ± 0.2	96.5 ± 0.2	97.8 ± 0.4	98.2 ± 0.2
PNF-60PTMG	74.3 ± 2.1	94.9 ± 0.2	97.3 ± 0.1	98.3 ± 0.2	98.7 ± 0.3
PNF-70PTMG	90.4 ± 0.6	97.9 ± 0.1	98.6 ± 0.2	99.0 ± 0.1	99.2 ± 0.1

[a]Elastic property is demonstrated by the shape recovery ratio at 200% strain using a cyclic tensile test.

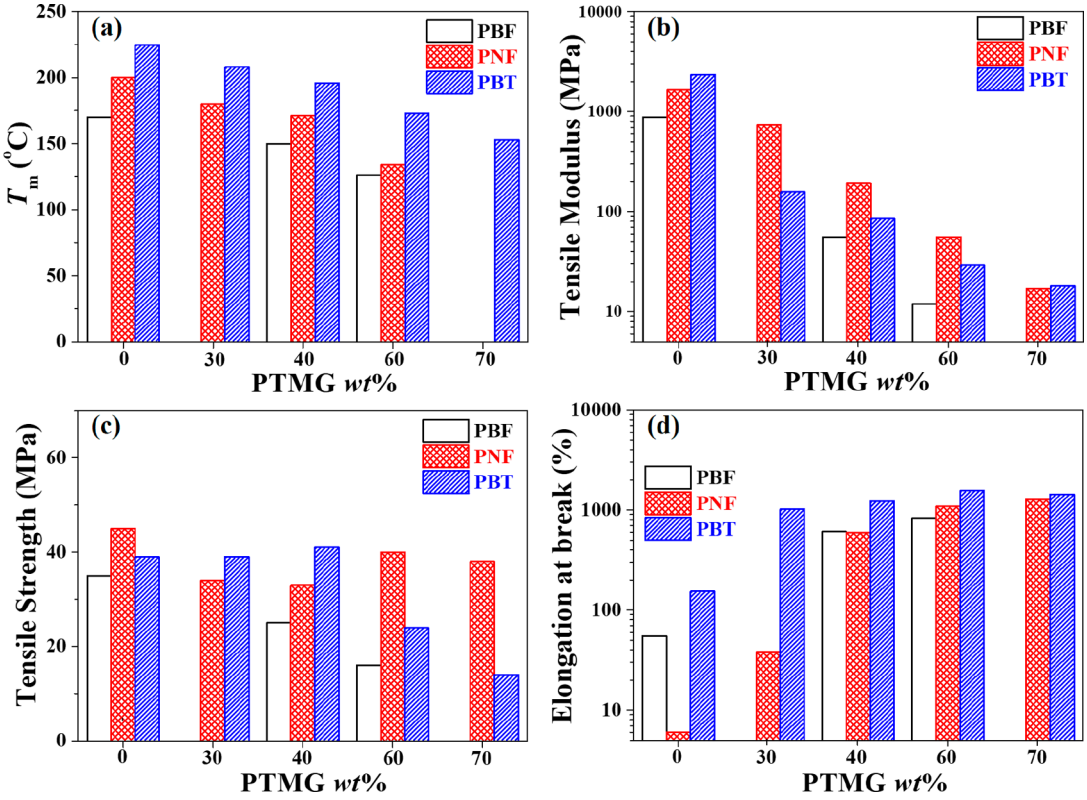

Figure 8. Comparison of properties of TPEEs with different hard segments: (a) melting temperature, (b) tensile modulus, (c) tensile strength, and (d) elongation at break.

and the results are listed in Table 3. PBF and PBT have similar δ_s values, which are slightly higher than that of PNF. In addition, according to the literature,[38] the δ_s of PTMG is 8.5 $(J\ cm^{-3})^{1/2}$. Therefore, the differences between PNF, PBF, and PBT to that of PTMG are 11.8, 14.4, and 14.2 $(J\ cm^{-3})^{1/2}$, respectively. Since all three $\Delta\delta_s$ values are higher than 10 $(J\ cm^{-3})^{1/2}$, phase separation should occur in all three TPEEs.[39] Moreover, an evaluation based on the theoretical calculation of $\Delta\delta_s$ indicates that the degree of microphase separation for the three TPEEs is in the following order: PBF−PTMG ≈ PBT−PTMG > PNF−PTMG.

On the other hand, the kinetic factor, such as crystallization, will induce and accelerate the microphase separation of the two thermodynamically immiscible components.[40] As a result, TPEEs actually contain four phases, the crystalline hard segment, the amorphous hard segment, the amorphous soft segment, and a mixture of amorphous hard and soft segments.[41−44] For traditional TPEEs such as PBT−PTMG, three thermal transitions can be observed. One is the melting temperature for the crystalline hard segment, and the other two are the glass transition temperatures for the amorphous hard segment and the amorphous soft segment.[44,45] The two glass transition temperatures usually shift and merge to form a broad peak with the increasing thermodynamical miscibility of the two amorphous domains.

In the case of PNF−PTMG, only a single glass transition temperature is observed in DSC analysis, located at 37 °C (Figure 2 and Table 2) for PNF-30PTMG, which is smaller than that of PNF (68 °C). No obvious glass transition temperature can be identified for PNF−PTMG with a greater amount of PTMG. Therefore, we performed DMA testing to investigate the main relaxation (α relaxation) of PNF−PTMG so that the microphase separation behavior could be revealed.

Figure 4 demonstrates the DMA curves for PNF and PNF−PTMG, and the α relaxation temperatures (T_α) obtained from tan δ curves are listed in Table 4. PNF−PTMG have only one broad peak in the tan δ curves, which indicates that they contain only one amorphous phase consisting of both amorphous PTMG and amorphous PNF. Although they are thermodynamically immiscible as predicted by the calculation of δ_s, PNF−PTMG has the lowest degree of microphase separation; these two amorphous domains are able to mix with each other to form a single phase. Similarly, Ji and co-workers pointed out that amorphous PBF is miscible with the PTMG soft segment in PBF−PTMG,[14] in spite of a relatively large $\Delta\delta_s$. Therefore, PNF−PTMG have only two phases instead of four. One phase is the crystalline PNF hard segment domain,

DOI: 10.1021/acssuschemeng.8b01105
ACS Sustainable Chem. Eng. 2018, 6, 9893−9902

and the other phase is the mixture of amorphous PTMG and amorphous PNF domain. As a result, the microphase separation in PNF−PTMG is mainly induced by the kinetic factor, namely, the crystallization of PNF. In addition, analysis using the Fox equation[46] also illustrates that a large amount of amorphous PTMG obstructs the kinetic factor that promotes microphase separation, thus PTMG and PNF form a miscible mixture with good compatibility (see Supporting Information).

It is worth noting that PNF-30PTMG showed a slightly different storage modulus profile compared with the other samples (Figure 4c). The storage modulus of PNF-30PTMG sharply decreased at 60 °C and then increased again with a small peak centered at about 90 °C. This is because PNF-30PTMG was subject to a cold crystallization process in this temperature range, which has been clearly demonstrated in the DSC curve in Figure 2. As a result, the storage modulus of the sample increased slightly. However, for all other samples, they have no cold crystallization; therefore, their storage moduli did not increase.

Small-angle X-ray scattering (SAXS) was performed to further reveal the microphase separation and microstructure of PNF−PTMG. Figure 5 displays the SAXS profiles of PNF−PTMG. First, the one-dimensional curves (Figure 5a) show that the peak becomes broader and its intensity decreases when its maximum value moves to a lower q with increasing PTMG content, where q is the scattering vector of the peak. Moreover, except for PNF-30PTMG, only one main peak can be observed for PNF−PTMG, indicating the absence of long-range order for these samples. Information about changes in the long period (L), as well as continuous gradient change in the flexible segment components, can be calculated directly by the Bragg's law: $L = 2\pi/q_{max}$. The characteristic variations of the L come from changes of the amorphous layer (l_a) and the crystalline layer (l_c), with a relationship among the three: $L = l_a + l_c$. A broad peak can be observed in the q range of 0.5−0.7 nm^{-1}, corresponding to a length scale of 10 nm. The values of L are within 10.6−11.6 nm from PNF-40PTMG to PNF-70PTMG. Thus, the separated microphase of PNF−PTMG has a similar size of about 11 nm. However, we are unable to decide whether it is the amorphous or the crystalline thickness that is read from the correlation function without prior knowledge of crystallinity. Second, the two-dimensional scattering patterns with the characteristics of disordered microphase separation indicated that all PNF−PTMG samples have a similar phase structure, as clearly shown in Figure 5b.[47] The intensity of the scattering ring gradually becomes more disperse and weaker from PNF-30PTMG to PNF-70PTMG, showing that the segmentation becomes more disordered with the increasing PTMG amount, which is correlated with the loss of heterogeneity. This result is in good agreement with that from DMA analysis that the PNF and PTMG have increased compatibility with the increasing of the PTMG amount. In other words, better crystallization induces a higher degree of phase separation for PNF−PTMG, and as a result, the scattering ring became stronger and clearer.

Summarizing, we can conclude that although PNF and PTMG have a certain amount of thermodynamical immiscibility, increasing the amount of PTMG impedes the kinetic factor, namely, the crystallization of PNF. This would hinder the microphase separation, and as a result, the degree of microphase separation decreases in PNF−PTMG with a high amount of PTMG.

Mechanical and Elastic Properties of PNF−PTMG. After detailed investigations on the molecular structure, thermal properties, and microphase separation, we performed tensile testing to study the mechanical and elastic properties of PNF−PTMG. The representative tensile strain−stress curves are presented in Figure 6. The relevant results are summarized in Table 5. It can be clearly seen that with the increase of PTMG amount, the tensile modulus (E) of PNF−PTMG decreases but the elongation at break (ε_b) increases, while the tensile strength (σ_t) remains unchanged. Similar trends can be observed in other TPEE systems.[14−16] Decreasing of E is due to the fact that the rigidity of the material is ascribed to the crystalline hard segment. Incorporation of the flexible PTMG soft segment breaks the crystalline structure of the hard segment and results in a decrease of E. On the contrary, the flexible PTMG soft segment increases the toughness of the material, which results in a dramatic increase of ε_b. All PNF−PTMG have similar σ_t because of the strain-hardening effect, especially for the three samples with a high amount of PTMG. Actually, the first two samples with a low amount of PTMG, namely, PNF-30PTMG and PNF-40PTMG, behave more like thermoplastic polyesters. PNF-30PTMG is too brittle to show yield (see Figure 6), while PNF-40PTMG has an obvious yield behavior. More importantly, PNF−PTMG has decreased yield stress (σ_y) and increased yield strain (ε_y) when the PTMG amount increases from 40 to 50 wt%, indicating a gradually faded away yield behavior, which disappears when the PTMG amount is 60 wt% or more. Therefore, the rest of the three samples behave like a thermoplastic elastomer.

In order to study the rubbery behavior of the rest three samples, the elastic deformability and reversibility of them were investigated by cyclic tensile testing. The representative cyclic tensile testing strain−stress curves are showed in Figure 7, and the shape recovery ratio (R_r) at 200% strain during five successive cycles are listed in Table 6. In the first place, the shape recovery ratio in the first cycle ($R_r(1)$) increases gradually from 57% to over 90% when the PTMG amount increases from 50 to 70 wt%, indicating an enhanced elastic property. This is because the elasticity of the material is provided by the flexible PTMG soft segment. In the second place, rearrangement in the crystalline microphase can predicte that the strain−stress curve in the second cycle will be much more compliant than that observed in the first cycle.[48] As expected, the loading−unloading cycle curves hover at a stable fixed trajectory from the second cycle, which can also be observed in common elastomers. Finally, it can be seen that PNF-50PTMG exhibits an obvious yield point, and the mini-neck drawn phenomenon can be observed after the cyclic tensile testing (Figure S6). However, PNF-60PTMG and PNF-70PTMG showed slight or even no neck drawn phenomenon after cyclic tensile testing.

Properties Comparison. As a novel TPEE, comparing its properties to the existing ones is important to better evaluate the potential of its application. PBT−PTMG, the classical TPEE known as Hytrel, and its analog based on FDCA, namely, PBF−PTMG, are selected for comparison with PNF−PTMG. The three TPEEs have the same PTMG soft segments but different hard segments. Figure 8 shows a comparison of the thermal and mechanical properties of the three TPEEs. The relevant data for PNF, PBF−PTMG, and PBT−PTMG are adopted from previous studies.[14,26,32,49] First, PNF−PTMG has a higher T_m than that of PBF−PTMG but a lower T_m than that of PBT−PTMG, regardless of the amount

DOI: 10.1021/acssuschemeng.8b01105
ACS Sustainable Chem. Eng. 2018, 6, 9893−9902

of PTMG (Figure 8a). This is because PNF has a moderate T_m among the three hard segments. Moreover, PBT-70PTMG shows a fairly high T_m of over 150 °C, while PNF-70PTMG becomes totally amorphous without a T_m. This is because PBT has a better crystallization ability than that of PNF. Second, although PNF has a lower E than PBT, after incorporation of PTMG soft segment with up to 60 wt%, the resulting PNF−PTMG has a higher E than PBT−PTMG (Figure 8b). When it comes to the σ_t, when the PTMG amount is 40 wt% or lower, PNF−PTMG has a relative smaller σ_t than PBT−PTMG. However, when the PTMG amount is 60 wt% or higher, PNF−PTMG has a significantly larger σ_t than PBT−PTMG. Finally, PNF is more brittle than both PBF and PBT. However, when the PTMG soft segment is introduced to form PNF−PTMG, it has a largely enhanced toughness comparable to both PBF−PTMG and PBT−PTMG. With a 40 wt% or more amount of PTMG, all three TPEEs have a similar elongation at break of around 1000%. On the basis of the results above, it is reasonable to conclude that PNF−PTMG has similar thermal properties and better mechanical properties compared with those of both PBF−PTMG and PBT−PTMG. The novel bio-based TPEE has great potential to be used as an alternative to classical TPEEs such as PBT−PTMG.

CONCLUSIONS

In this work, by combining NPG and FDCA to produce PNF with both a high melting temperature and crystallization ability, we have identified PNF as a promising hard segment for the development of novel bio-based TPEE with superior performance comparable to the commercial and petroleum-based TPEE. It was found that incorporation of the PTMG soft segment would decrease the melting temperature, glass transition temperature, and tensile modulus of PNF−PTMG but would increase the elongation at break and shape recovery ratio of PNF−PTMG, while the tensile strength remained unchanged. Therefore, the thermal and mechanical properties of PNF−PTMG can be readily manipulated by varying the ratio between the hard and soft segments, which is similar to the traditional TPEEs. The resulting PNF−PTMG showed high performance because it can induce microphase separation due to the thermodynamical immiscibility between PNF and PTMG and, more importantly, the crystallization of PNF. Thus, PNF plays a very important role not only in inducing microphase separation but also in serving as a strong physical cross-link so that novel bio-based TPEE can be obtained. With an excellent comprehensive performance, PNF−PTMG has potential applications and is expected to be used in various fields as an alternative to traditional TPEEs.

ASSOCIATED CONTENT

Supporting Information

The Supporting Information is available free of charge on the ACS Publications website at DOI: 10.1021/acssuschemeng.8b01105.

Details of sample treatment, characterization methods, and figures related to GPC, FT-IR, XRD, Flory equation, Fox equation, and sample bars (PDF)

AUTHOR INFORMATION

Corresponding Authors

*E-mail: liufei@nimte.ac.cn.

*E-mail: nahaining@nimte.ac.cn.

ORCID

Fei Liu: 0000-0002-7848-5226

Haining Na: 0000-0001-8067-9962

Notes

The authors declare no competing financial interest.

ACKNOWLEDGMENTS

The authors are grateful for financial support from the National Natural Science Foundation of China (NSFC, 51503217), the Zhejiang Province Public Welfare Project (2017C31081), the National Key Research and Development Program of China (2017YFE0102300), and the Open Project Program of MOE Key Laboratory of Macromolecular Synthesis and Functionalization, Zhejiang University (2016MSF001).

REFERENCES

(1) Spontak, R. J.; Patel, N. P. Thermoplastic elastomers: fundamentals and applications. *Curr. Opin. Colloid Interface Sci.* **2000**, *5*, 333−340.

(2) Foss, R.; Jacobson, H.; Cripps, H.; Sharkey, W. Block and Graft Copolymers of Pivalolactone. II. ABA and ABA-g-A Copolymers with Dienes. *Macromolecules* **1976**, *9* (2), 373−374.

(3) Foss, R. P.; Jacobson, H. W.; Cripps, H. N.; Sharkey, W. H. Block and Graft Copolymers of Pivalolactone. 4. Triblock and Block-Graft Copolymers from Pivalolactone and Isoprene. *Macromolecules* **1979**, *12* (6), 1210−1216.

(4) Holden, G.; Legge, N. R.; Quirk, R. P.; Schroeder, H. E. *Thermoplastic Elastomers*, 2nd ed; Gardner: Cincinnati, OH, 1993.

(5) Holden, G.; Kricheldorf, H. R.; Quirk, R. P. *Thermoplastic Elastomers*, 3rd ed; Hanser Gardner: Cincinnati, OH, 2004.

(6) Konyukhova, E. V.; Neverov, V. M.; Godovsky, Y. K.; Chvalun, S. N.; Soliman, M. Deformation of Polyether-Polyester Thermoelastoplastics: Mechanothermal and Structural Characterisation. *Macromol. Mater. Eng.* **2002**, *287* (4), 250−265.

(7) Zhu, Y.; Romain, C.; Williams, C. K. Sustainable polymers from renewable resources. *Nature* **2016**, *540* (7633), 354−362.

(8) Bolton, J. M.; Hillmyer, M. A.; Hoye, T. R. Sustainable Thermoplastic Elastomers from Terpene-Derived Monomers. *ACS Macro Lett.* **2014**, *3* (8), 717−720.

(9) Shin, J.; Lee, Y.; Tolman, W. B.; Hillmyer, M. A. Thermoplastic Elastomers Derived from Menthide and Tulipalin A. *Biomacromolecules* **2012**, *13* (11), 3833−3840.

(10) Papageorgiou, G. Z.; Papageorgiou, D. G.; Terzopoulou, Z.; Bikiaris, D. N. Production of bio-based 2,5-furan dicarboxylate polyesters: Recent progress and critical aspects in their synthesis and thermal properties. *Eur. Polym. J.* **2016**, *83*, 202−229.

(11) Sousa, A. F.; Vilela, C.; Fonseca, A. C.; Matos, M.; Freire, C. S. R.; Gruter, G.-J. M.; Coelho, J. F. J.; Silvestre, A. J. D. Biobased polyesters and other polymers from 2,5-furandicarboxylic acid: a tribute to furan excellency. *Polym. Chem.* **2015**, *6* (33), 5961−5983.

(12) Szymczyk, A. Structure and properties of new polyester elastomers composed of poly(trimethylene terephthalate) and poly(ethylene oxide). *Eur. Polym. J.* **2009**, *45* (9), 2653−2664.

(13) Piesowicz, E.; Paszkiewicz, S.; Szymczyk, A. Phase Separation and Elastic Properties of Poly(Trimethylene Terephthalate)-blockpoly(Ethylene Oxide) Copolymers. *Polymers* **2016**, *8* (7), 237.

(14) Zhou, W.; Zhang, Y.; Xu, Y.; Wang, P.; Gao, L.; Zhang, W.; Ji, J. Synthesis and characterization of bio-based poly(butylene furandicarboxylate)-b-poly(tetramethylene glycol) copolymers. *Polym. Degrad. Stab.* **2014**, *109*, 21−26.

(15) Wu, B.; Xu, Y.; Bu, Z.; Wu, L.; Li, B.-G.; Dubois, P. Biobased poly(butylene 2,5-furandicarboxylate) and poly(butylene adipate-co-butylene 2,5-furandicarboxylate)s: From synthesis using highly purified 2,5-furandicarboxylic acid to thermo-mechanical properties. *Polymer* **2014**, *55* (16), 3648−3655.

DOI: 10.1021/acssuschemeng.8b01105
ACS Sustainable Chem. Eng. 2018, 6, 9893−9902

(16) Kwiatkowska, M.; Kowalczyk, I.; Kwiatkowski, K.; Szymczyk, A.; Rosłaniec, Z. Fully biobased multiblock copolymers of furan-aromatic polyester and dimerized fatty acid: Synthesis and characterization. *Polymer* **2016**, *99*, 503−512.
(17) Wang, G.; Jiang, M.; Zhang, Q.; Wang, R.; Zhou, G. Biobased multiblock copolymers: Synthesis, properties and shape memory performance of poly(ethylene 2,5-furandicarboxylate)-b-ly(ethylene glycol). *Polym. Degrad. Stab.* **2017**, *144*, 121−127.
(18) Jiang, M.; Liu, Q.; Zhang, Q.; Ye, C.; Zhou, G. A Series of Furan-Aromatic Polyesters Synthesized via Direct Esterification Method Based on Renewable Resources. *J. Polym. Sci., Part A: Polym. Chem.* **2012**, *50* (5), 1026−1036.
(19) Papageorgiou, G. Z.; Tsanaktsis, V.; Papageorgiou, D. G.; Exarhopoulos, S.; Papageorgiou, M.; Bikiaris, D. N. Evaluation of polyesters from renewable resources as alternatives to the current fossil-based polymers. Phase transitions of poly(butylene 2,5-furandicarboxylate). *Polymer* **2014**, *55* (16), 3846−3858.
(20) Papageorgiou, G. Z.; Tsanaktsis, V.; Bikiaris, D. N. Synthesis of poly(ethylene furandicarboxylate) polyester using monomers derived from renewable resources: thermal behavior comparison with PET and PEN. *Phys. Chem. Chem. Phys.* **2014**, *16* (17), 7946−7958.
(21) Coleman, D. Block Copolymers: Copolymerization of Ethylene Terephthalate and Polyoxyethylene Glycols. *J. Polym. Sci.* **1954**, *14* (73), 15−28.
(22) Veenstra, H.; Hoogvliet, R. M.; Norder, B.; De Boer, A. P. Microphase Separation and Rheology of a Semicrystalline Poly(ether-ester) Multiblock Copolymer. *J. Polym. Sci., Part B: Polym. Phys.* **1998**, *36* (11), 1795−1804.
(23) Hong, P.; Chung, W.; Hsu, C. Crystallization kinetics and morphology of poly(trimethylene terephthalate). *Polymer* **2002**, *43* (11), 3335−3343.
(24) Tsanaktsis, V.; Terzopoulou, Z.; Exarhopoulos, S.; Bikiaris, D. N.; Achilias, D. S.; Papageorgiou, D. G.; Papageorgiou, G. Z. Sustainable, eco-friendly polyesters synthesized from renewable resources: preparation and thermal characteristics of poly(dimethylpropylene furanoate). *Polym. Chem.* **2015**, *6* (48), 8284−8296.
(25) deJong, E.; Dam, M. A.; Sipos, L.; Gruter, G. J. M., Furandicarboxylic Acid (FDCA), A Versatile Building Block for a Very Interesting Class of Polyesters. In *241st National Meeting and Exposition of the American-Chemical-Society*; Smith, P.; Gross, R., Eds.; Amer. Chemical Soc.: Anaheim, CA, 2012; Vol. *1105*, pp 1−13.
(26) Genovese, L.; Lotti, N.; Siracusa, V.; Munari, A. Poly(Neopentyl Glycol Furanoate): A Member of the Furan-Based Polyester Family with Smart Barrier Performances for Sustainable Food Packaging Applications. *Materials* **2017**, *10* (9), 1028.
(27) Papageorgiou, G. Z.; Papageorgiou, D. G.; Tsanaktsis, V.; Bikiaris, D. N. Synthesis of the bio-based polyester poly(propylene 2,5-furan dicarboxylate). Comparison of thermal behavior and solid state structure with its terephthalate and naphthalate homologues. *Polymer* **2015**, *62*, 28−38.
(28) Zhu, J.; Cai, J.; Xie, W.; Chen, P.-H.; Gazzano, M.; Scandola, M.; Gross, R. A. Poly(butylene 2,5-furan dicarboxylate), a Biobased Alternative to PBT: Synthesis, Physical Properties, and Crystal Structure. *Macromolecules* **2013**, *46* (3), 796−804.
(29) McCarthy, S.; Meijs, G.; Gunatillake, P. Synthesis, characterization, and stability of poly[(alkylene oxide) ester] thermoplastic elastomers. *J. Appl. Polym. Sci.* **1997**, *65* (7), 1319−1332.
(30) Yave, W.; Szymczyk, A.; Yave, N.; Roslaniec, Z. Design, synthesis, characterization and optimization of PTT-b-PEO copolymers: A new membrane material for CO2 separation. *J. Membr. Sci.* **2010**, *362* (1−2), 407−416.
(31) Yokouchi, M.; Sakakibara, Y.; Chatani, Y.; Tadokoro, H.; Tanaka, T.; Yoda, K. Structures of 2 Crystalline Forms of Poly(butylene terephthalate) and Reversible Transition between Them by Mechanical Deformation. *Macromolecules* **1976**, *9* (2), 266−273.
(32) Liu, F.; Zhang, J.; Wang, J.; Na, H.; Zhu, J. Incorporation of 1,4-cyclohexanedicarboxylic acid into poly(butylene terephthalate)-b-poly (tetramethylene glycol) to alter thermal properties without compromising tensile and elastic properties. *RSC Adv.* **2015**, *5* (114), 94091−94098.
(33) Knox, B.; Weigmann, H.; Scott, M. Interations of Non-aqueous Solvents with Textile Fibers 5. Application of Solubility Parameter Concept to Polyester Fiber-solvent Interactions. *Text. Res. J.* **1975**, *45* (3), 203−217.
(34) Deslandes, N.; Bellenger, V.; Jaffiol, F.; Verdu, J. Solubility Parameter of a Polyester Composite Material. *J. Appl. Polym. Sci.* **1998**, *69* (13), 2663−2671.
(35) Pospiech, D.; Gottwald, A.; Jehnichen, D.; Friedel, P.; John, A.; Harnisch, C.; Voigt, D.; Khimich, G.; Bilibin, A. Determination of interaction parameters of block copolymers containing aromatic polyesters from solubility parameters obtained from solution viscosities. *Colloid Polym. Sci.* **2002**, *280* (11), 1027−1037.
(36) Adamska, K.; Voelkel, A.; Berlinska, A. The solubility parameter for biomedical polymers-Application of inverse gas chromatography. *J. Pharm. Biomed. Anal.* **2016**, *127*, 202−206.
(37) Small, P. Some Factors Affecting the Solubility of Polymers. *J. Appl. Chem.* **1953**, *3* (2), 71−80.
(38) Van Krevelen, D. W. *Properties of Polymers*; Elsevier: Amsterdam, 1972.
(39) Greenhalgh, D.; Williams, A.; Timmins, P.; York, P. Solubility parameters as predictors of miscibility in solid dispersions. *J. Pharm. Sci.* **1999**, *88* (11), 1182−1190.
(40) Watts, A.; Kurokawa, N.; Hillmyer, M. A. Strong, Resilient, and Sustainable Aliphatic Polyester Thermoplastic Elastomers. *Biomacromolecules* **2017**, *18* (6), 1845−1854.
(41) Lilaonitkul, A.; West, J.; Cooper, S. Propertires of Poly-(tetramethylene oxide)-poly(tetramethylene terephthalate) Block Polymers. *J. Macromol. Sci., Part B: Phys.* **1976**, *12* (4), 563−597.
(42) Gabrielse, W.; Soliman, M.; Dijkstra, K. Microstructure and phase behavior of block copoly(ether ester) thermoplastic elastomers. *Macromolecules* **2001**, *34* (6), 1685−1693.
(43) Litvinov, V.; Bertmer, M.; Gasper, L.; Demco, D.; Blumich, B. Phase composition of block copoly(ether ester) thermoplastic elastomers studied by solid-state NMR techniques. *Macromolecules* **2003**, *36* (20), 7598−7606.
(44) Szymczyk, A.; Senderek, E.; Nastalczyk, J.; RoslanieC, Z. New multiblock poly(ether-ester)s based on poly(trimethylene terephthalate) as rigid segments. *Eur. Polym. J.* **2008**, *44* (2), 436−443.
(45) Seymour, R.; Overton, J.; Corley, L. Morphological Characterization of Polyester-based Elastoplastics. *Macromolecules* **1975**, *8* (3), 331−335.
(46) Fox, T. G. *Bull. Am. Phys. Soc.* **1956**, *1*, 123.
(47) Zhang, J.; Deubler, R.; Hartlieb, M.; Martin, L.; Tanaka, J.; Patyukova, E.; Topham, P. D.; Schacher, F. H.; Perrier, S. Evolution of Microphase Separation with Variations of Segments of Sequence-Controlled Multiblock Copolymers. *Macromolecules* **2017**, *50* (18), 7380−7387.
(48) Soccio, M.; Lotti, N.; Gigli, M.; Finelli, L.; Gazzano, M.; Munari, A. Reactive blending of poly(butylene succinate) and poly(triethylene succinate): characterization of the copolymers obtained. *Polym. Int.* **2012**, *61* (7), 1163−1169.
(49) Zhang, J.; Liu, F.; Wang, J.; Na, H.; Zhu, J. Synthesis of poly(butylene terephthalate)-poly(tetramethylene glycol) copolymers using terephthalic acid as starting material: A comparation between two synthetic strategies. *Chin. J. Polym. Sci.* **2015**, *33* (9), 1283−1293.

DOI: 10.1021/acssuschemeng.8b01105
ACS Sustainable Chem. Eng. 2018, 6, 9893−9902